Multimode Fibre-based Optical-resolution Photoacoustic Endo-microscopy with a Real-valued Intensity Transmission Matrix

Tianrui Zhao, Sebastien Ourselin, Tom Vercauteren, Wenfeng Xia

School of Biomedical Engineering and Imaging Sciences, King's College London, 4th Floor, Lambeth Wing St Thomas' Hospital, London SE1 7EH, United Kingdom

tianrui.zhao@kcl.ac.uk

Abstract: We present the development of a forward-viewing optical-resolution photoacoustic endo-microscopy probe based on a multimode fibre via high-speed wavefront shaping. High-resolution 3D photoacoustic microscopy images of carbon fibres and red blood cells were obtained.

1. Introduction

Photoacoustic (PA) imaging has emerged as a non-invasive hybrid imaging modality by providing distinct spectroscopic signatures of tissues at highly scalable spatial resolution and imaging depth, with various pre-clincial and clinical applications in many clinical fields such as cell biology, neurology and oncology [1–3]. However, PA imaging suffers from rapid reduction of signal strength with the increase of tissue penetration depth due to strong optical attenuation of biological tissue. PA endoscopy has demonstrated good potential to extend the scope of PA imaging for imaging deep tissues [4–6]. In this work, we developed a highly miniaturised forward-reviewing optical-resolution PA endomicroscopy probe based on a 140 μm-diameter multimode fibre via a high-speed method for wavefront shaping.

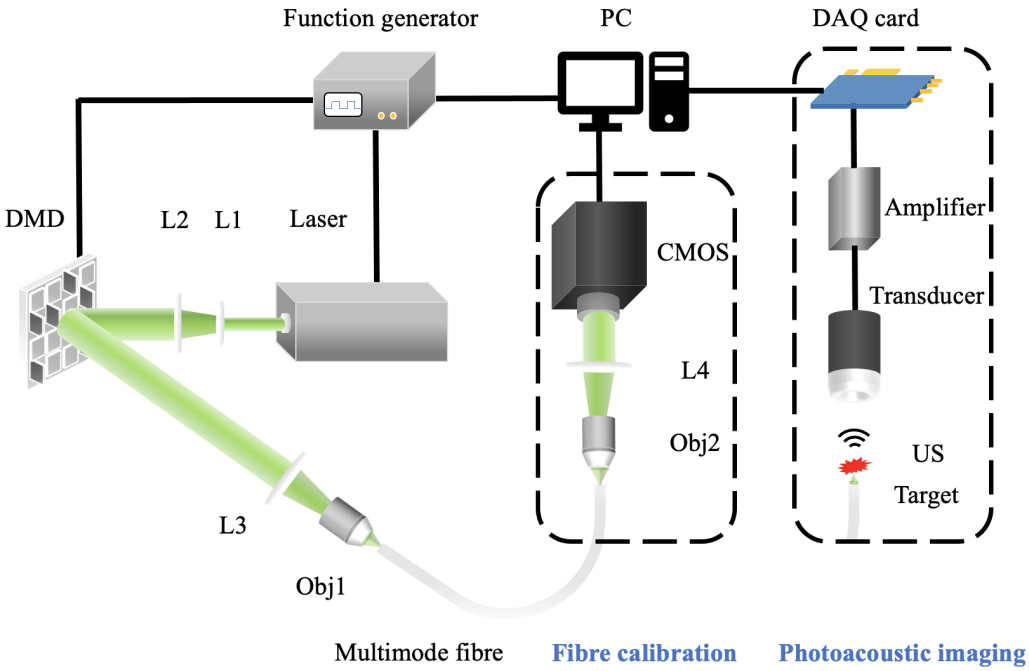

Fig. 1. Schematic illustration of the experimental setup including a fibre characterisation module and a photoacoustic imaging module. DMD, digital micromirror device; L1-L4, tube lenses; Obj1-2, 20x objectives; CMOS, camera; US, ultrasound.

2. Methods and materials

2.1. Real-valued intensity transmission matrix

Fibre charaterisation was based on a real-valued intensity transmission matrix (RVITM) method previously developed in our group [7, 8]. Briefly, the relationship between the input and output light intensities was modelled as:

$$\begin{bmatrix} I_1^1 & \cdots & I_1^{2N} \\ \vdots & \ddots & \vdots \\ I_m^1 & \cdots & I_m^{2N} \end{bmatrix} = RVITM \bullet [H_1, H_2], \tag{1}$$

In the characterisation step, we employed a series of binary patterns $[H_1, H_2]$ as input whilst the corresponding output speckles were recorded. A Hadamard matrix H $\in$ (-1, +1) with dimensions of N x N was used to construct two binary matrices $H_1 = (H+1)/2$ and $H_2 = (-H+1)/2$. A RVITM characterising the intensity change between each input mode and output mode were then calculated as:

$$RVITM = \begin{bmatrix} 2I_1^1 - I_1^1 & \cdots & 2I_1^{2N} - I_1^1 \\ \vdots & \ddots & \vdots \\ 2I_m^1 - I_m^1 & \cdots & 2I_m^{2N} - I_m^1 \end{bmatrix} \bullet [H, -H]^T, \tag{2}$$

where I_m^k is the intensity at the m^{th} output position when the k^{th} binary Hadamard pattern is displayed as input, $k \in (0, \cdots, 2N)$. Optimal DMD patterns for light focusing and scanning through the fibre were obtained by switching 'ON' micromirrors with a higher RVITM value than a preset threshold.

2.2. Experiment

The experimental setup for fibre characterisation and PA imaging is shown in Fig. 1. A diode-pumped solid state laser emitting at 532 nm with a pulse duration of 2 ns (SPOT-10-200-532) was used as the light source. A DMD (DLP7000) was used to project binary patterns onto the proximal end of a MMF (Ø100 µm, 0.29 NA, 20 cm, Newport) via a tube lens (AC254-050-A-ML, Thorlabs) and an objective (20×, RMS20X, Thorlabs). A region of the DMD covering 128x128 micromirrors was used for light modulation in this study. For fibre characterisation, a CMOS camera (C11440-22CU01, Hamamatsu Photonics) was used to capture the output speckles after an objective (20×, RMS20X, Thorlabs) and a tube lens (AC254-0100-A-ML, Thorlabs).

After the fibre characterisation, the characterisation module was replaced by the photoacoustic imaging module as shown in the dash box in Fig. 1. A silica plano-concave lens (LC4210, Thorlabs) was attached onto a piezoelectric transducer (50 MHz, V358) for acoustic focusing at the optical focal plane in front of the fibre distal end. Imaging target was placed at the optical focal plane with water for acoustic coupling. An optical focus was scanned across a circular region with a diameter of 100 μm by light modulations with pre-determined optimal DMD patterns, whilst ultrasound signals were recorded by a data acquisition card (M4i.4420, Spectrum) after amplification (SPA.1411, Grosshansdorf). Each PA image comprised 200×200 pixels and the scanning step was set to be 0.5 μm. Synchronization of the laser pulsing, data acquisition and DMD display was controlled by a waveform generator (33600A, Keysight, Santa Rosa) and a customised MATLAB program.

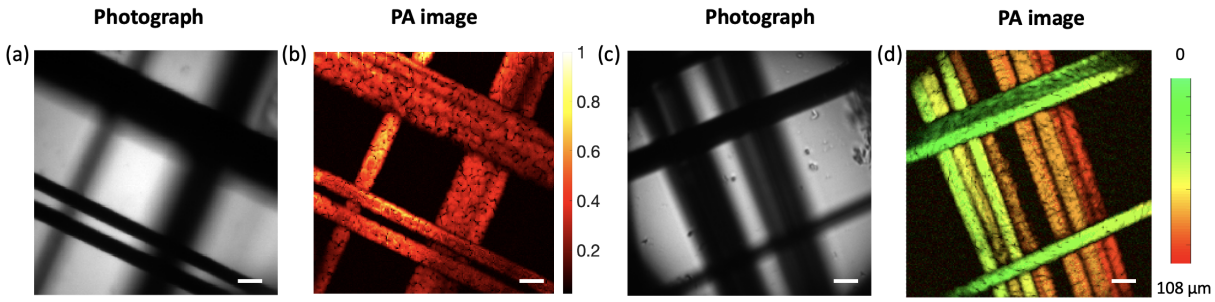

Fig. 2. Examples of photoacoustic (PA) images of of carbon fibre networks. (b) maximum intensity projection along the depth direction, and (d) a 3D rendering with depth information colour-coded. (a) and (c) are the corresponding photographs. Scale: 10 μm.

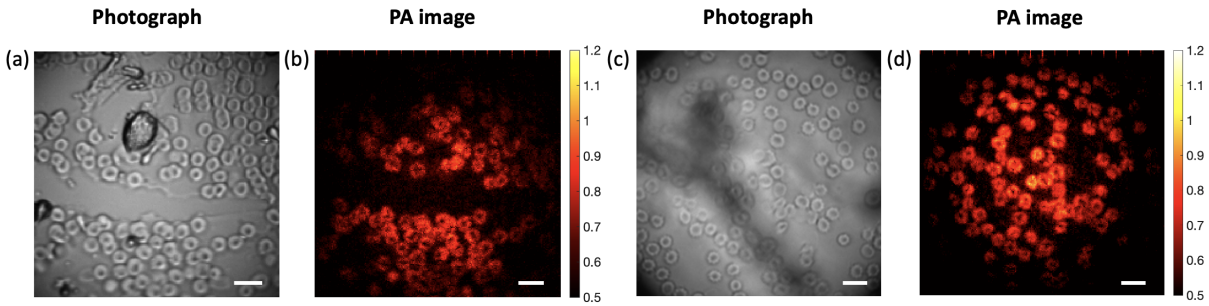

Fig. 3. Examples of photoacoustic (PA) images of mouse red blood cells (b,d), and their corresponding photographs (a,c). PA images are maximum intensity projections along the depth direction and were normalised to their maximum values and displayed on a linear scale. Scale: 10 μm.

3. Results and discussion

The multimode fibre was characterised to transmit and scan a focused laser beam with a diameter of $\sim$1.4 μm. With the DMD running at 23 kHz, it cost $\sim$1.7 s for the acquisition of each frame. Fig 2 shows a maximum intensity projection of PA image of mouse red blood cells, and a 3D PA image of a carbon fibre network with colour-coded depth information. In the future, an all-optical fibre-optic forward-viewing photoacoustic endomicroscopy probe will be developed with ultrasound detection via a Fabry-Perot resonator coated at the distal end of a single-mode fibre [9, 10]. Potential of this ultra-thin PA endoscopy probe for guiding minimally invasive procedures will be exploited.

Funding

Wellcome Trust (203148/Z/16/Z, WT101957); Engineering and Physical Sciences Research Council (NS/A000027/1, NS/A000049/1); Medtronic/Royal Academy of Engineering Chair (RCSRF1819/7/34).

References

1. Paul Beard. Biomedical photoacoustic imaging. *Interface focus*, 1(4):602–631, 2011.
2. Murad Omar, Juan Aguirre, and Vasilis Ntziachristos. Optoacoustic mesoscopy for biomedicine. *Nature Biomedical Engineering*, 3(5):354–370, 2019.
3. Lihong V Wang. Multiscale photoacoustic microscopy and computed tomography. *Nature photonics*, 3(9):503–509, 2009.
4. Tianrui Zhao, Adrien E Desjardins, Sebastien Ourselin, Tom Vercauteren, and Wenfeng Xia. Minimally invasive photoacoustic imaging: Current status and future perspectives. *Photoacoustics*, 16:100146, 2019.
5. P Hajireza, W Shi, and RJ Zemp. Label-free in vivo fiber-based optical-resolution photoacoustic microscopy. *Optics letters*, 36(20):4107–4109, 2011.
6. Rehman Ansari, Edward Z Zhang, Adrien E Desjardins, and Paul C Beard. All-optical forward-viewing photoacoustic probe for high-resolution 3d endoscopy. *Light: Science & Applications*, 7(1):1–9, 2018.
7. Tianrui Zhao, Sebastien Ourselin, Tom Vercauteren, and Wenfeng Xia. Seeing through multimode fibers with real-valued intensity transmission matrices. *Optics Express*, 28(14):20978–20991, 2020.
8. Tianrui Zhao, Sebastien Ourselin, Tom Vercauteren, and Wenfeng Xia. High-speed photoacoustic-guided wavefront shaping for focusing light in scattering media. *Optics Letters*, (In press).
9. James A Guggenheim, Jing Li, Thomas J Allen, Richard J Colchester, Sacha Noimark, Olumide Ogunlade, Ivan P Parkin, Ioannis Papakonstantinou, Adrien E Desjardins, Edward Z Zhang, et al. Ultrasensitive plano-concave optical microresonators for ultrasound sensing. *Nature Photonics*, 11(11):714–719, 2017.
10. Tianrui Zhao, Lei Su, and Wenfeng Xia. Optical ultrasound generation and detection for intravascular imaging: a review. *Journal of healthcare engineering*, 2018, 2018.